Received: 27 April 2018 | Revised: 31 July 2018 | Accepted: 3 September 2018 | Published on: 23 September 2018

DOI: 10.1002/joc.5861

International Journal of Climatology RMetS

RESEARCH ARTICLE

Projected changes in drought across the wheat belt of southeastern Australia using a downscaled climate ensemble

Puyu Feng[1,2] | De Li Liu[2,3] | Bin Wang[2] | Cathy Waters[4] | Mingxi Zhang[2,5] | Qiang Yu[1,5,6]

[1]School of Life Sciences, Faculty of Science, University of Technology Sydney, Sydney, New South Wales, Australia

[2]NSW Department of Primary Industries, Wagga Wagga Agricultural Institute, Wagga Wagga, New South Wales, Australia

[3]Climate Change Research Centre and ARC Centre of Excellence for Climate Extremes, University of New South Wales, Sydney, New South Wales, Australia

[4]NSW Department of Primary Industries, Orange Agricultural Institute, Orange, New South Wales, Australia

[5]State Key Laboratory of Soil Erosion and Dryland Farming on the Loess Plateau, Northwest A&F University, Yangling, China

[6]College of Resources and Environment, University of Chinese Academy of Science, Beijing, China

Correspondence
Puyu Feng, School of Life Sciences, Faculty of Science, University of Technology Sydney, PO Box 123, Broadway, Sidney 2007, New South Wales, Australia.
Email: puyu.feng@student.uts.edu.au

Funding information
National Basic ResearchProgram of China, Grant/Award Number: 2012CB955304

Drought is viewed as a naturally recurring phenomenon in many Australian agricultural systems. Identifying regional changes in frequency and severity of drought induced by climate change is required to develop regionally specific adaptation strategies. In this study, we provided a first look at the impacts of climate change on 21st century drought characteristics over the New South Wales wheat belt of southeastern Australia. These impacts were assessed from an ensemble of 28 statistical downscaled global climate models under representative concentration pathway (RCP8.5). A modified relative standardized precipitation and evapotranspiration index (rSPEI) at the seasonal scale (3 months) was used to analyse temporal and spatial changes in drought. Results indicated that there was a tendency towards more frequent and severe winter–spring droughts over the study area. Moreover, winter–spring drought prone areas were expected to expand from west to east. Until the end of the 21st century, more than half the wheat belt would be vulnerable to winter–spring drought. The combined effects of reduced precipitation and increased temperature during future winter and spring seasons were the main reasons causing these changes of drought. In addition, summer and autumn droughts would have both slight temporal and spatial changes across the study region. This study also revealed that traditionally dry areas would likely experience an increased frequency of drought compared to wetter areas when subjected to a same increase in temperature or decrease in precipitation. Furthermore, the western part of the wheat belt might be unsuitable for winter crops in the future, or at least exposed to an increased risk of variable yield and would require a gradual transformation which might include summer crops or pastures. Investments in cropping land should be focused on the east part of the wheat belt to achieve more consistent financial returns.

KEYWORDS
climate change, drought, rSPEI, southeastern Australia, spatio-temporal variations

1 | INTRODUCTION

Drought is a temporal and recurrent phenomenon, which originates from prolonged absence, shortage or unusual distribution of precipitation compared to the normal pattern. The occurrences of above-average temperature which lead to increased evaporation can also inevitably aggravate drought occurrence. Given a high level of confidence that climate change will lead to increased temperature and changed precipitation pattern (Field, 2012), drought conditions are likely to change greatly in many parts of the world (Ahmadalipour *et al*., 2016; Spinoni *et al*., 2017). However, as drought is often a period- and region-specific disaster (Wilhite, 1993), it is difficult to identify the occurrence and the severity of a drought event based on simple and fixed standards of precipitation or temperature anomalies in a particular region (Morid *et al*., 2007; Trinh *et al*., 2017). Therefore, there is an urgent requirement to develop appropriate methods to identify expected changes of drought conditions at regional scales, which is critical for land managers to develop mitigation and adaptation strategies.

The Coupled Model Intercomparison Project phase 5 (CMIP5, https://cmip.llnl.gov/cmip5/) is a powerful tool to analyse the projections of 21st century climate change. A number of physical-based global climate models (GCMs) are available for obtaining future drought projections based on the assumptions of the future economic development or associated greenhouse gas (GHG) emissions. As the real climate system is immensely complex, no single model is capable of describing its overall process adequately even in a particular region (Tebaldi and Knutti, 2007). Recent studies tend to use multiple GCMs to assess future drought conditions. For example, Dai (2012) managed to project worldwide drought conditions until the end of 21st century based on 14 GCMs under representative concentration pathways 4.5 (RCP4.5). The results of Dai (2012) indicated severe droughts in the next few decades over many mid-latitude areas such as the eastern United States, Europe, and Australia, because of either increased evaporation and/or decreased precipitation. Ahmadalipour *et al*. (2016) used 21 CMIP5 GCMs to assess drought projections and revealed a significant increase in frequency and intensity of future summer droughts across the United States under RCP8.5. Kirono *et al*. (2011) demonstrated that there is a likely risk (more than 66% probability) of at least doubling drought frequency and an increase in drought affected areas in southeastern Australia by 2070 based on projections from 14 CMIP3 GCMs under SRES-A1B and A2 emission scenario. The use of multiple GCMs is considered to reduce model uncertainties and provide more reliable future projections (Mpelasoka *et al*., 2018).

The importance of applying appropriate indices for drought assessment has been addressed in a number of studies (Heim, 2002; Mishra and Singh, 2010). Evaluating drought characteristics systematically and comprehensively at regional scales may be problematic using a series of values. In the past few decades, researchers have managed to develop numerous drought indices by integrating climate factors including precipitation, temperature, and evapotranspiration into a single value. The most widely used drought indices include the Palmer drought severity index (PDSI), the self-calibrating PDSI (Wells *et al*., 2004), the moisture anomaly index (Z-index) (Palmer, 1965), and the standardized precipitation index (SPI; Thomas *et al*., 1993). Generally, these indices improve the identification of the onset of a drought event as well as the measurement of drought severity, which then allows an assessment of spatial and temporal features of drought in various areas. However, most drought indices have a fixed temporal range. For example, PDSI can only capture droughts on timescales of more than 9 months (Guttman, 1998; Lloyd-Hughes and Saunders, 2002), and it cannot be used to detect dry periods at shorter timescales. The SPI is designed in a way that can identify droughts at timescales from small (to one month) up large (to 72 month) periods. However, the SPI is calculated using precipitation alone, and it fails to take into account the important contribution of temperature via evaporation (Nicholls, 2004). Another drought index, the standardized precipitation evapotranspiration index (SPEI; Vicente-Serrano *et al*., 2010), has been developed to overcome this shortcoming of the SPI. The SPEI is calculated based on the difference between precipitation and potential evapotranspiration (PET), thereby accounting for energy balance and temperature changes as well as precipitation, but also retaining positive traits of the SPI. While the SPEI is a recently developed drought index, it has been widely used and received considerable attention in numerous studies to analyse drought condition (e.g., Wang *et al*., 2015; Gao *et al*., 2017). However, the SPEI still has a shortcoming. For example, a given amount of precipitation and PET at a wet station that produces a negative SPEI may produce a positive SPEI at a dry station. In another word, dryness and wetness are relative to the local historical average rather than the absolute difference between precipitation and PET at a certain station. Therefore, the SPEI has limitations for spatial comparison. In this study, we introduced a relative SPEI (rSPEI) which is based on regional average rather than local conditions, to improve the performance of the original SPEI.

Australia is the driest inhabited continent in the world and drought is an expected feature of the Australian climate (Ummenhofer *et al*., 2009). Drought causes large agricultural losses in Australia. For example, in southeastern Australia, drought reduced the agricultural Gross National Product by around 30% in 1994, 2002, and 2006 (Kirono *et al*., 2011). It is likely that climate change will further exaggerate drought impacts in this region (BOM and CSIRO, 2016). The main objectives of this study are to (a) use rSPEI as an indicator of drought to examine the spatial and temporal characteristics of future drought occurrence across major farming regions of southeastern Australia until the end of 21st century from an ensemble of 28 CMIP5 GCMs; (b) identify the major climatic factors which contribute to the change of drought frequency under future climate change; (c) identify suitable adaptation measures to mitigate the negative impacts of drought in the study area.

2 | MATERIALS AND METHOD

2.1 | Study domain description

The domain of the study is the New South Wales (NSW) wheat belt (141.0°–152.0°E, 28.5°–36.1°S) of southeastern

Australia, which covers an area of 360,000 km^2 (Figure 1) (Liu *et al*., 2014). There is an east–west gradient in both elevation and precipitation/temperature across the study area. The eastern part of the wheat belt consists of mountains with an elevation up to 1,100 m and the western areas are mainly plains. Average temperature ranges from 11 °C in the southeast to 20 °C in the northwest and average annual precipitation ranges from 1,000 mm in the southeast to 200 mm in the southwest (Figure 2). Overall, the eastern part of the wheat belt is wet and cold, while the western part is dry and warm. In NSW wheat belt, winter crops commonly include wheat and canola, while summer crops are mainly sorghum and maize. In particular, wheat is the most important commodity which contributes to 15% of the gross value of agricultural production in NSW (http://www.abs.gov.au/Agriculture).

2.2 | Climate data

In this study, the monthly gridded data of 28 GCMs (Table 1) were acquired from CMIP5. These GCMs are from different climate modelling institutions all over the world. Detailed descriptions of these GCMs can be found at https://cmip.llnl.gov/cmip5/.

Raw GCMs are unable to produce regional scale projections, because they are normally at coarse spatial resolutions (100–300 km grid spacing). Thus, we downscaled raw GCMs data to weather observation stations using a weather-generator based statistical downscaling approach which was developed by NSW Department of Primary Industries at Wagga Wagga Agricultural Institute (NWAI-WG) and has been described by Liu and Zuo (2012). This approach has been frequently used in recent climate change research (e.g., Anwar *et al*., 2015; Wang *et al*., 2016; He *et al*., 2017) which allows daily data of meteorological factors from monthly gridded GCMs to be derived. It can also correct biases in the raw GCMs. Briefly, the first step of the downscaling procedure was to interpolate the monthly gridded data for each weather station (931 stations in the NSW wheat belt, Figure 1) using inverse distance weighted (IDW) method (Bartier and Keller, 1996). A bias correction method was applied in this step to enable the resulting monthly station data to match with observed data (downloaded from Scientific Information for Land Owners patched point data set, http://www.longpaddock.qld.gov.au/silo/ppd/index.php) using quantile–quantile (QQ) mapping technique (Zhang, 2005; Zhang, 2007). Second, the bias-corrected monthly values were disaggregated to daily data through the modified WGEN weather generator (Richardson and Wright, 1984). Further details of procedures and results of this method can be found in Liu and Zuo (2012).

In GCMs data set, four representative concentration pathways (RCP2.6, RCP4.5, RCP6.0, and RCP8.5) are available, which describe four possible future climates based on future concentrations of GHGs. RCP8.5 represents the most serious condition with continuous rising emissions throughout the 21st century. Studies have shown that trends in GHGs concentrations since 2000 agree better with those projected by RCP8.5 than any other scenarios (Peters *et al*., 2011; Diffenbaugh and Field, 2013). Therefore, RCP8.5 was utilized in this study as it has projections which are most likely to be achieved in the future (Ribeiro *et al*., 2016).

2.3 | Relative SPEI

The original SPEI is based on climatic water balance and allows for the contribution of temperature in drought assessment. It uses the difference between precipitation (P) and evapotranspiration (PET) as parameter to characterize drought. It is a standardized index for which a value of 0 represents the median P-PET (i.e., normal conditions), while dry conditions are denoted by negative values (i.e., −2 for extremely dry) and wet conditions are denoted by positive values (i.e., 2 for extremely wet). Generally, a value of <−1

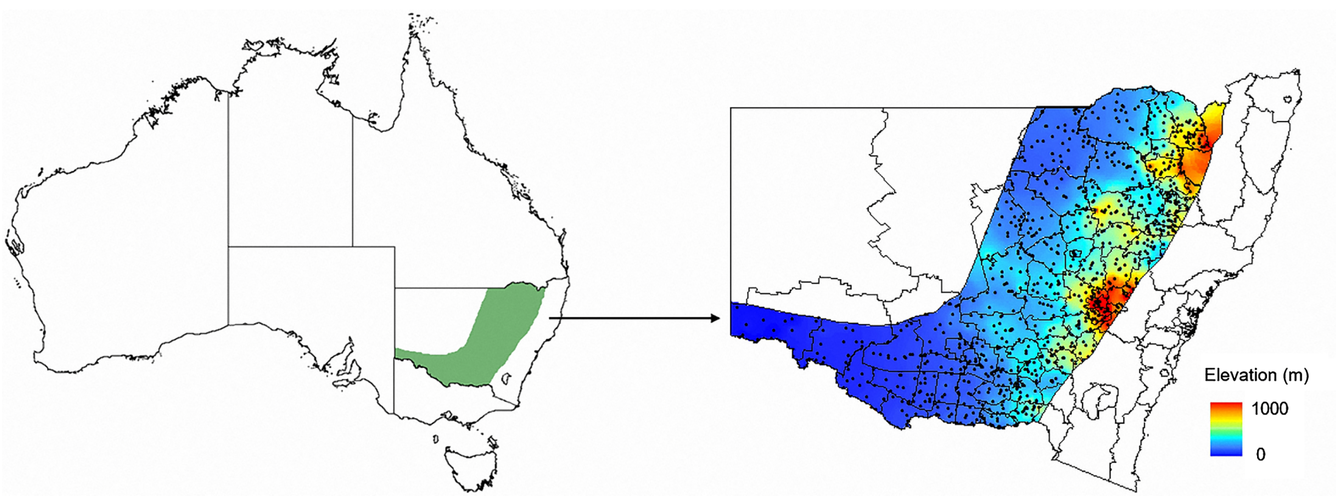

FIGURE 1 The study area is located in the New South Wales wheat belt of southeastern Australia. Black points are the locations of 931 weather stations used in the study [Colour figure can be viewed at wileyonlinelibrary.com]

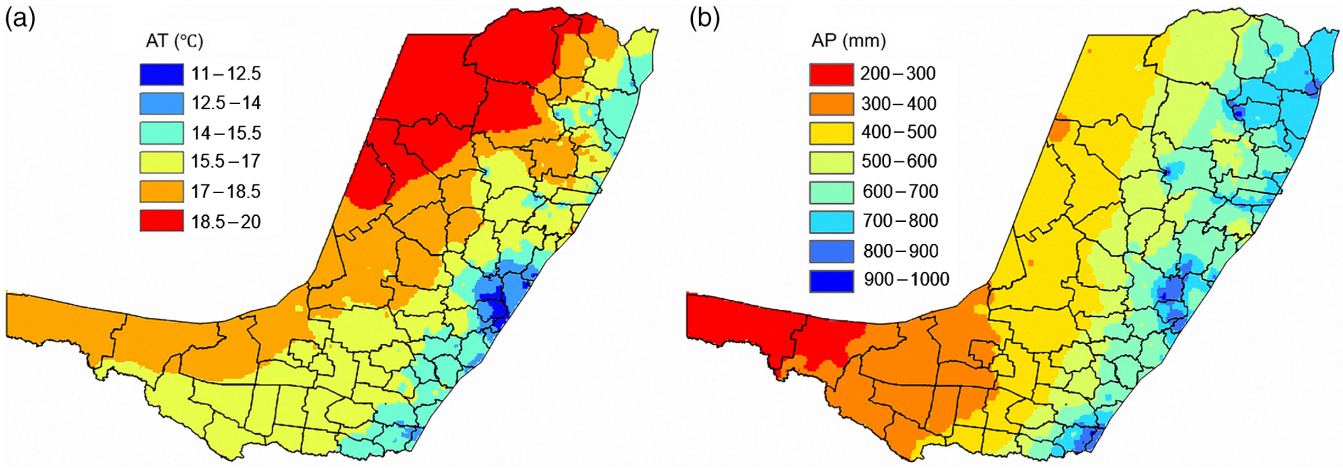

FIGURE 2 Spatial distributions of (a) annual mean temperature (AT) and (b) mean annual precipitation (AP) over the New South Wales wheat belt of southeastern Australia during 1961–1990 [Colour figure can be viewed at wileyonlinelibrary.com]

TABLE 1 List of 28 GCMs under RCP8.5 future climate scenarios used in this study for statistical downscaling outputs of 931 stations over the New South Wales wheat belt of southeastern Australia

Model ID	Name of GCM	Abbr. of GCM	Institute ID	Country
01	BCC-CSM1.1	BC1	BCC	China
02	BCC-CSM1.1(m)	BC2	BCC	China
03	BNU-ESM	BNU	GCESS	China
04	CanESM2	CaE	CCCMA	Canada
05	CCSM4	CCS	NCAR	United States
06	CESM1(BGC)	CE1	NSF-DOE-NCAR	United States
07	CMCC-CM	CM2	CMCC	Europe
08	CMCC-CMS	CM3	CMCC	Europe
09	CSIRO-Mk3.6.0	CSI	CSIRO-QCCCE	Australia
10	EC-EARTH	ECE	EC-EARTH	Europe
11	FIO-ESM	FIO	FIO	China
12	GISS-E2-H-CC	GE2	NASA GISS	United States
13	GISS-E2-R	GE3	NASA GISS	United States
14	GFDL-CM3	GF2	NOAA GFDL	United States
15	GFDL-ESM2G	GF3	NOAA GFDL	United States
16	GFDL-ESM2M	GF4	NOAA GFDL	United States
17	HadGEM2-AO	Ha5	NIMR/KMA	Korea
18	INM-CM4	INC	INM	Russia
19	IPSL-CM5A-MR	IP2	IPSL	France
20	IPSL-CM5B-LR	IP3	IPSL	France
21	MIROC5	MI2	MIROC	Japan
22	MIROC-ESM	MI3	MIROC	Japan
23	MIROC-ESM-CHEM	MI4	MIROC	Japan
24	MPI-ESM-LR	MP1	MPI-M	Germany
25	MPI-ESM-MR	MP2	MPI-M	Germany
26	MRI-CGCM3	MR3	MRI	Japan
27	NorESM1-M	NE1	NCC	Norway
28	NorESM1-ME	NE2	NCC	Norway

is viewed as drought condition. In addition, the SPEI can be calculated on different timescales according to specific aims.

Conceptually, one SPEI value indicates the deviation of P-PET at a given station for a given period from "normal condition." This raises a problem. For a wet station and a dry station within a region, a given amount of P-PET that produces negative SPEI (say −1) at the wet station might supposedly produce positive SPEI at the dry station. So, the relative aridity condition remains uncertain between stations when using the original SPEI. Dubrovsky *et al*. (2008) ever used a relative SPI to make comparisons of absolute drought conditions. Here, we introduced the rSPEI which improved the calculation of the original SPEI and can be applied to spatial analysis.

The process of calculating the original SPEI mainly consists of two steps. (a) fit the P-PET series into a log-logistic distribution to acquire parameters; (b) convert the distribution into a normal distribution to determine SPEI values. In this case, the same P-PET series is used in both steps. For the calculation of rSPEI, we created a reference P-PET series by aggregating all monthly P-PET totals of the 931 stations,

$$\overline{D}_j = \overline{P}_j - \overline{\mathrm{PET}_j}, \tag{1}$$

where $\overline{P}_j$, $\overline{\mathrm{PET}_j}$, and $\overline{D}_j$ are the averaged total precipitation, the accumulated PET and the deficit of *j*th month at the 931 weather stations. Then, the averaged accumulated P-PET at *k*-month scale is calculated by

$$\begin{cases} \overline{X}^k_{i,j} = \sum_{l=13-k+j}^{12} \overline{D}_{i-1,l} + \sum_{l=1}^{j} \overline{D}_{i,l} & \text{if } j<k \\ \overline{X}^k_{i,j} = \sum_{l=j-k+1}^{j} \overline{D}_{i,l} & \text{if } j \geq k, \end{cases} \tag{2}$$

where is the accumulated P-PET at *k*-month scale in *j*th month of *i*th year; is the monthly P-PET in *l*th month of *i*th year. The parameters for the log-logistic distribution were acquired according to this reference series. Then, the values of the rSPEI relative to the reference distribution function were acquired for each station. In this study, the rSPEI was calculated for a 3-month time period in order to investigate seasonal drought attributes. This above process enabled us to compare the P-PET deviation for each location using the distribution function that indicated the climate optimum of the given region rather than that of the individual location. A comparison between the rSPEI and the SPEI values is shown in Figure S1, Supporting Information.

2.4 | Evaluation of drought characteristics

Figure 3 illustrates the whole process of this study. We assessed future drought characteristics from three aspects: temporal changes, spatial changes, and major drivers of these changes.

2.4.1 | Temporal changes

We assessed the likely changes of drought severity across the wheat belt. As the rSPEI values represent the severity of drought, analysing the time series of the rSPEI values for each station can reveal temporal changes in drought. Two methods, that is, the Mann–Kendall trend test and the Sen's slope, were used. The Mann–Kendall trend test, which is often used to assess trends in hydroclimatological time series (Hamed and Ramachandra Rao, 1998; Lutz *et al*., 2016; Serrano-Notivoli *et al*., 2018), was applied to test the significance of trends on the time series of the rSPEI for each station. On the other hand, the trend of a climate variable may not be assessed to be statistically significant while it might be of practical interest (Shahid, 2010; Sheikhy *et al*., 2017). Therefore, in our study, we also applied linear trend analysis on rSPEI time series using the Sen's slope (Sen, 1968) which could provide a robust estimation of trend. In addition, these two methods were both performed using the R package "trend" (Pohlert, 2018).

2.4.2 | Spatial changes

Different zones of the study area are characterized with rather different climate conditions (Figure 2). Thus, some zones might be more vulnerable to drought compared to others. These zones are defined as drought prone zones. A zone is identified as drought prone zone where there is a high drought frequency value. Drought frequency (DF, %) indicates the number of drought events occurring for a given period (Spinoni *et al*., 2013). Specified thresholds of DF are usually needed to identify the drought prone zone for different areas. Many studies (Wilhelmi and Wilhite, 2002; Sonmez *et al*., 2005; Patel *et al*., 2007) have defined the thresholds to filter drought prone areas, mainly ranging from 20 to 30%. In this study, we chose the upper value of the threshold (30%) because Australia is typically a dry continent. Seasonal drought events (rSPEI < -1) of each weather station were first counted for four 30-year periods (1961–1990, 2011–2040, 2041–2070, and 2071–2100) and then the DFs were calculated. The DFs were then interpolated for each grid cell (~3 km) using IDW method. Areas with more than 30% of seasonal drought events were then identified for each period and each season.

2.4.3 | Major drivers of the changes of drought

A descriptive statistical analysis was conducted using a least-squared multiple linear regression model between the changes in DF (%, Figure S2) and the changes in and precipitation (%, Figure S3) and temperature (°C, Figure S4). The regression allowed for a better evaluation of drought attributes, thereby providing useful insights into the nature and strength of the relationships.

3 | RESULTS

3.1 | Temporal changes in drought

Temporal variation of seasonal rSPEIs in all the 931 weather stations over the NSW wheat belt for the period of 1961–2100 are given in Figure 4. For each year, the rSPEI values projected by the 28 GCMs for the 931 stations were presented as a distribution. Distribution for each year was a complete presentation of seasonal drought conditions of the whole wheat belt based on the 28 GCMs. For example, in the spring of 1961, the concentrated position of the distribution was around 0.3. This meant that most weather stations

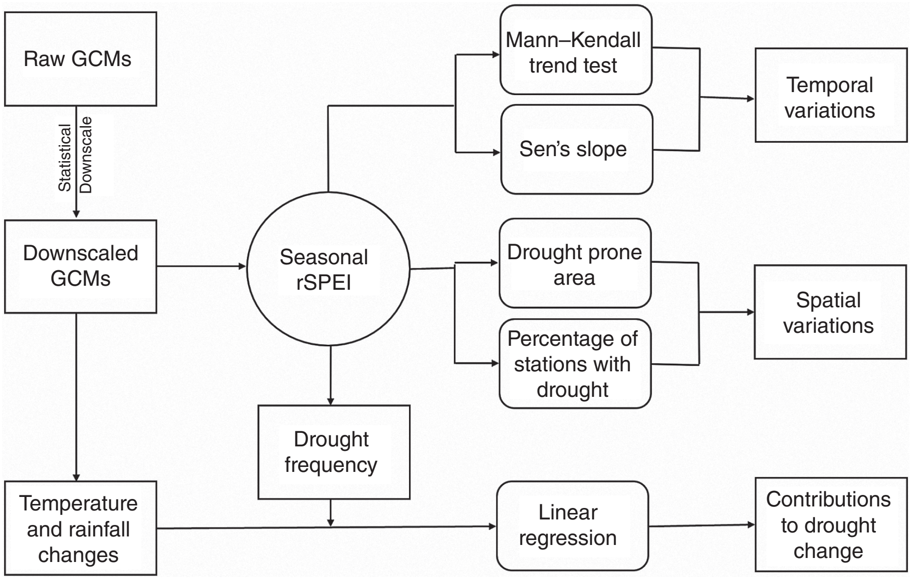

FIGURE 3 Framework of the procedures used in this study

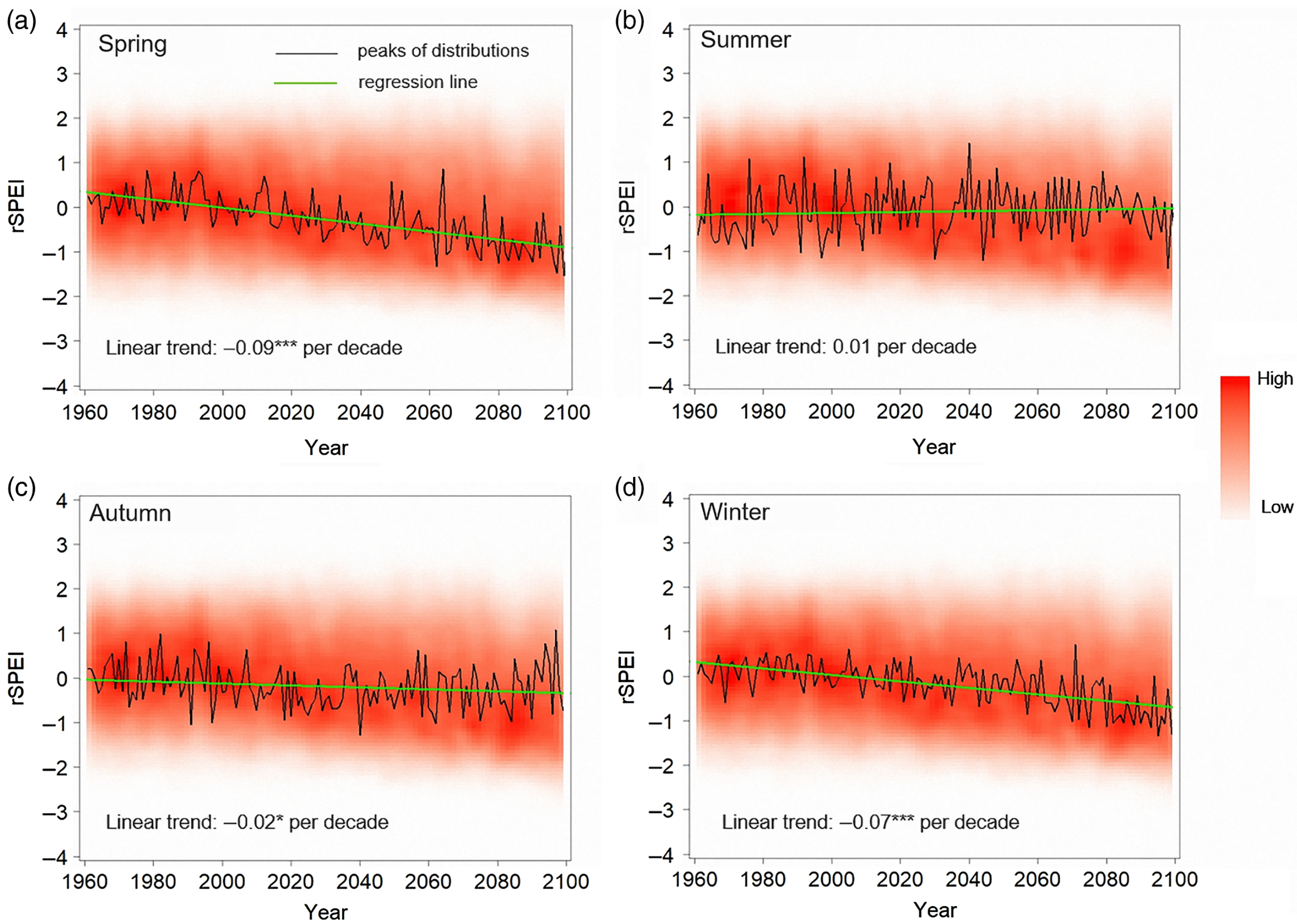

FIGURE 4 Changes in rSPEI values of the 931 weather stations in the New South Wales wheat belt of southeastern Australia during 1961–2100. Seasonal rSPEI values were first calculated for the 931 weather stations based on 28 GCMs. Then, for each year, seasonal rSPEI values from all the weather stations and GCMs were shown in a distribution. The red shaded area in the figure indicates the distribution of the rSPEI values for each year. The deeper the red colour, the more concentrated the distribution of the rSPEI values. Each distribution has a peak that indicates the most concentrated position. The black line captures the peaks of distributions of the rSPEI values for each year, so its change can to some extent represent the change in the distributions of the rSPEI values from the 931 weather stations based on 28 GCMs. The green line shows the linear trend of the rSPEI peaks. ***$p < .001$, **$p < .01$, *$p < .05$ [Colour figure can be viewed at wileyonlinelibrary.com]

had an rSPEI value of ~0.3, thus most of the wheat belt was in near normal climatic conditions. Therefore, changes in the distribution could then illustrate the overall change in drought condition for the entire wheat belt over the study period. Since the peak positions of every distribution could to some degree represent the concentrated distribution positions, we linked the peak positions using black lines to indicate trend. The distributions showed a significant ($p < .001$) decreasing trend in both spring and winter over the study period. The spring and winter periods decreased from 0.3 to nearly −1, indicating the majority of the wheat belt might experience future moderate drought conditions for these seasons. However, autumn and summer had relatively small trends and the rSPEI values for the majority of the wheat belt consistently fluctuated around 0. Therefore, in general, the wheat belt was expected to experience drier conditions in spring and winter but had little change in summer and autumn.

Figure 5 shows the changes of drought severity over the wheat belt in the future using rSPEI as a drought indicator. Trends of rSPEI were calculated through Sen's slope. The black triangles and circles indicate weather stations with a significant changing trend according to Mann–Kendall trend test. Generally, trends were consistent with the results indicated in Figure 4 and significant decreasing trends were projected in spring and winter for the entire wheat belt. Given that the rSPEI thresholds of −1, −1.5, and −2 indicate moderate, severe, and extreme drought condition, respectively, most of the wheat belt was likely to suffer a higher-level drought in spring and winter by the end of this century. While for summer and autumn, areas with slightly increased drought intensity were mainly located in the southwestern and northern areas, respectively. However, these trends were slight compared to those in spring and winter. In addition, northeastern areas during summers and southwestern areas during autumns were expected to experience decreased drought intensity.

3.2 | Spatial changes in drought

As the weather stations used in this study are relatively evenly distributed over the study area, the percentage of drought stations (rSPEI < −1) could be used to estimating the area size experiencing drought. Figure 6 illustrates the percentage of drought stations according to the rSPEI values of the 931 weather stations over the NSW wheat belt for the period of 1961–2100. Despite the inter-annual variability and GCM uncertainty, increasing trends were apparent in both winter and spring. About 40% of stations in the wheat belt could be expected to suffer continuous spring and winter

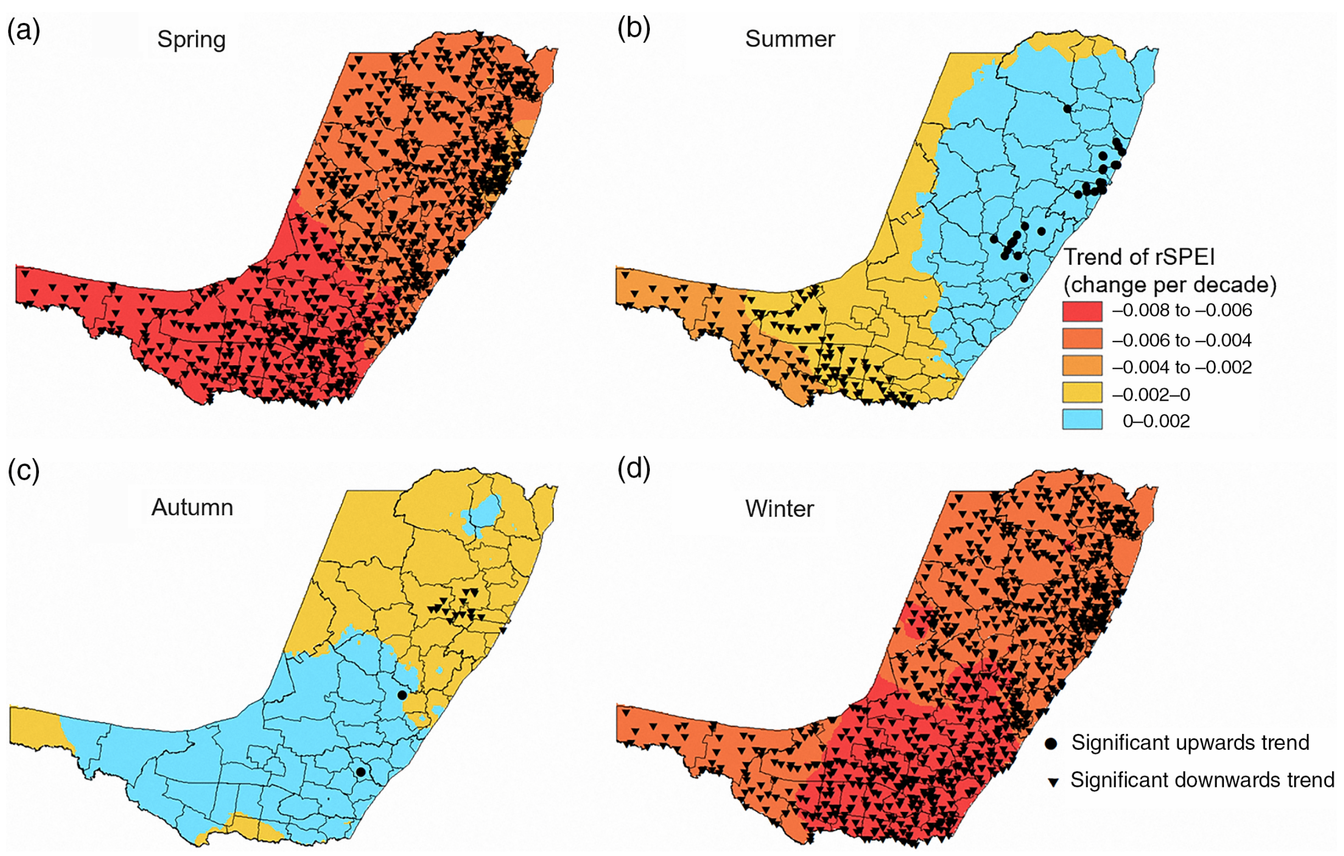

FIGURE 5 The trends of long-term seasonal drought across the New South Wales wheat belt of southeastern Australia in 2011–2100. The rSPEI is calculated for each of 28 GCMs and the average trend per decade (based on Sen's slope) from all downscaled GCMs is calculated for the 931 weather stations. We interpolated the trend of rSPEI using IDW method as the resolution of ~3 km. The black triangles and circles indicate stations with a significant changing trend based on the Mann-Kendall trend test ($|Z_S| > 1.96$) [Colour figure can be viewed at wileyonlinelibrary.com]

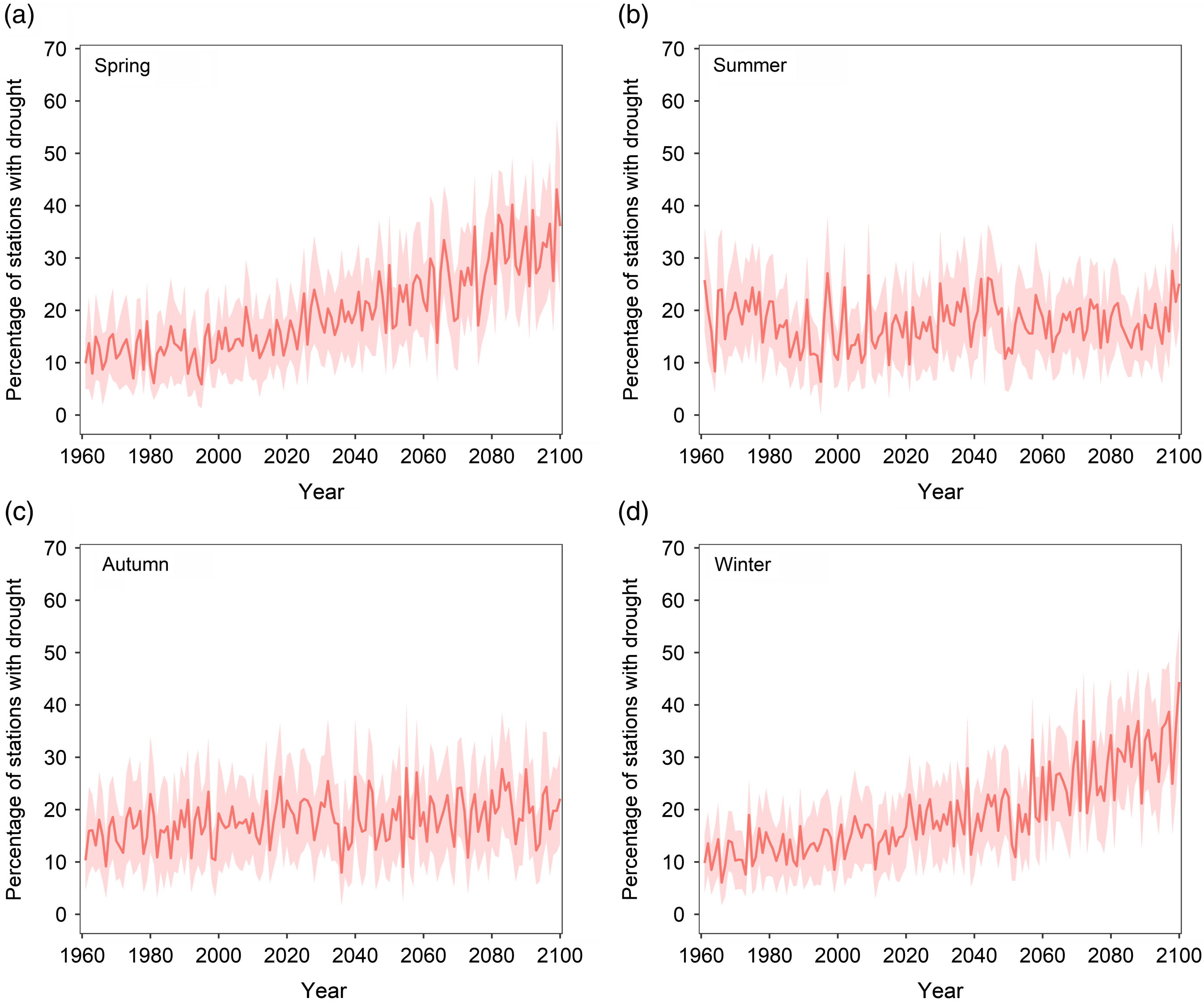

FIGURE 6 Percentage of stations with drought (rSPEI < −1) in the 931 weather stations across the New South Wales wheat belt of southeastern Australia for four seasons during 1961–2100. For each year, the percentage of stations with drought was calculated for each of 28 downscaled GCMs and multi-model ensemble mean values (red lines) were then plotted. The shading denotes the 95% confidence intervals for the 28 GCMs [Colour figure can be viewed at wileyonlinelibrary.com]

drought by the end of the 21st century. However, in summer and autumn, the percentages of drought stations fluctuated around 20% over time, with no obvious trend.

Drought prone areas were primarily in the western part of the wheat belt (Figure 7). This was particularly noticeable for spring and winter drought (Figure 6). For example, only a small area (14.6%, about 5.27×10^4 km^2) in the northwest of the wheat belt was drought vulnerable during 1961–1990 spring period. However, over time, the eastern limit expanded eastwards, and by the end of the 21st century over half (58.8%) of the wheat belt was at a high risk of experiencing spring drought. The winter drought prone area followed a similar expansion rate, but the area mainly expanded in the northern part of the wheat belt. Summer and autumn drought prone areas had slight changes over time.

3.3 | Major drivers of drought trends

The rSPEI calculations were based on precipitation and temperature, so changes in these variables would result in changes in the rSPEI. While the results of the rSPEI showed dramatic changes in future drought conditions, it was not clear if this was being driven by an increase in temperature, or by a decrease in precipitation. As different regions had different climates and aridity conditions, the primary factor might differ from location to location. In order to explore this possibility, seasonal changes in temperature and precipitation projected by the 28 downscaled GCMs were extracted for all weather stations in three 30-year periods (2011–2040, 2041–2070, and 2071–2100) compared to the baseline (1961–1990) (Figures S3 and S4). Based on elevation, the study area was divided into two zones (Figure 8), the eastern zone which is a mountainous area with an elevation of

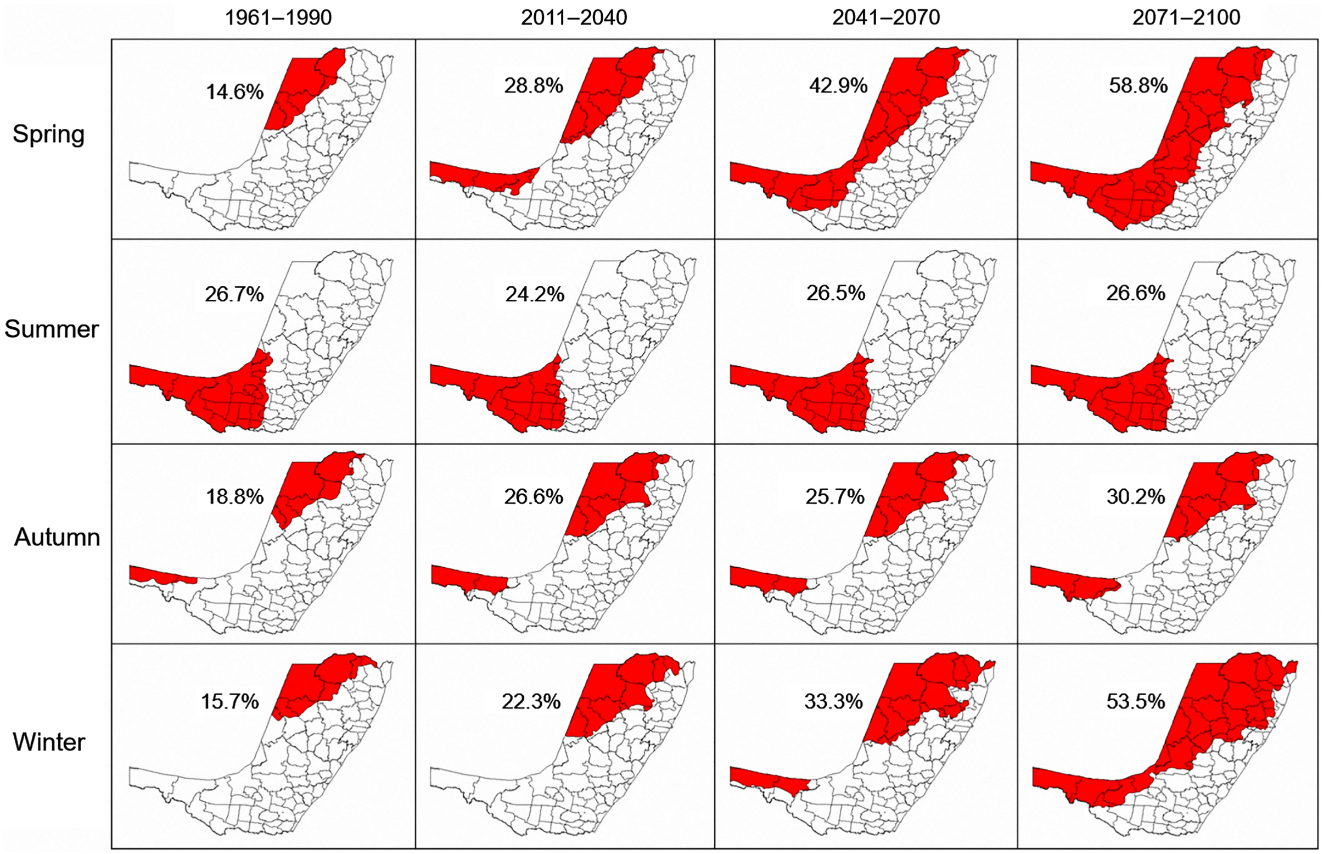

FIGURE 7 Changes in seasonal drought prone areas in the New South Wales wheat belt of southeastern Australia. Drought prone area is defined as an area with more than 30% of seasonal drought events (rSPEI < -1) for four 30-year periods (1961–1990, 2011–2040, 2041–2070, and 2071–2100). For each year and each season, multi-model ensemble means of rSPEI values were calculated for all stations based on the 28 downscaled GCMs and then percentages of <-1 values were calculated for each period. Then, the percentages were interpolated for each grid cell (~3 km). Areas with more than 30% of seasonal drought events are shown in red parts. The number in each plot denotes the proportion of the red area [Colour figure can be viewed at wileyonlinelibrary.com]

>300 m and the western zone which is mainly occupied by plains (<300 m). Climatically, the western zone is warm and dry, while the east is cold and wet (Figure 2). Spatial regression analysis was then applied between the changes in drought frequency (Figure S2) and the changes in temperature and precipitation using least-squares multiple regression (ΔDF = a*Δprecipitation (%) + b*Δtemperature (°C)) in both zones for each season and each period.

The R^2 (coefficient of determination) for each period and each season was higher in the western zone than the east (Figure 8). This meant that changes in seasonal precipitation and temperature were better able to explain DF change in the western zone. In addition, the magnitude of the regression coefficients (a, b) were also larger in the western zone than those in the east, which meant that the same decrease in precipitation or increase in temperature could result in a greater increase of DF in the western zone compared to the eastern.

Overall, temperature and precipitation changes had varying effects on drought in different seasons over time. For example, in spring and winter, DF increased greatly until 2100 with a small change in b but a large increase in a. Thus, although precipitation decreased (Figure S3) and temperature increased (Figure S4) over time simultaneously, the decrease in precipitation could be viewed as the major factor causing drought increase in spring and winter. However, in summer, both temperature and precipitation were expected to increase across the entire wheat belt, which leaded to a slight change in drought frequency. Therefore, both a and b decreased over time in summer. However, in autumn, a slight increase in precipitation was detected (Figure S3) but could not offset the effects caused by increased temperature. Thus, a also increased over time in autumn.

4 | DISCUSSION

This study investigated drought projections for the wheat belt of southeastern Australia using the ensemble of 28 statistical downscaled CMIP5 GCMs. The long-term seasonal drought trends (Figures 4 and 5) showed that the whole wheat belt was expected to suffer more severe spring and winter droughts. These findings are consistent with the results from CCIA (2015), which reported future decreased spring and winter precipitation in southern Australia. For example, more than half of 40 GCMs projected >15% decrease in winter–spring precipitation in our study area until the 2090s under RCP8.5 (CCIA, 2015). It should be

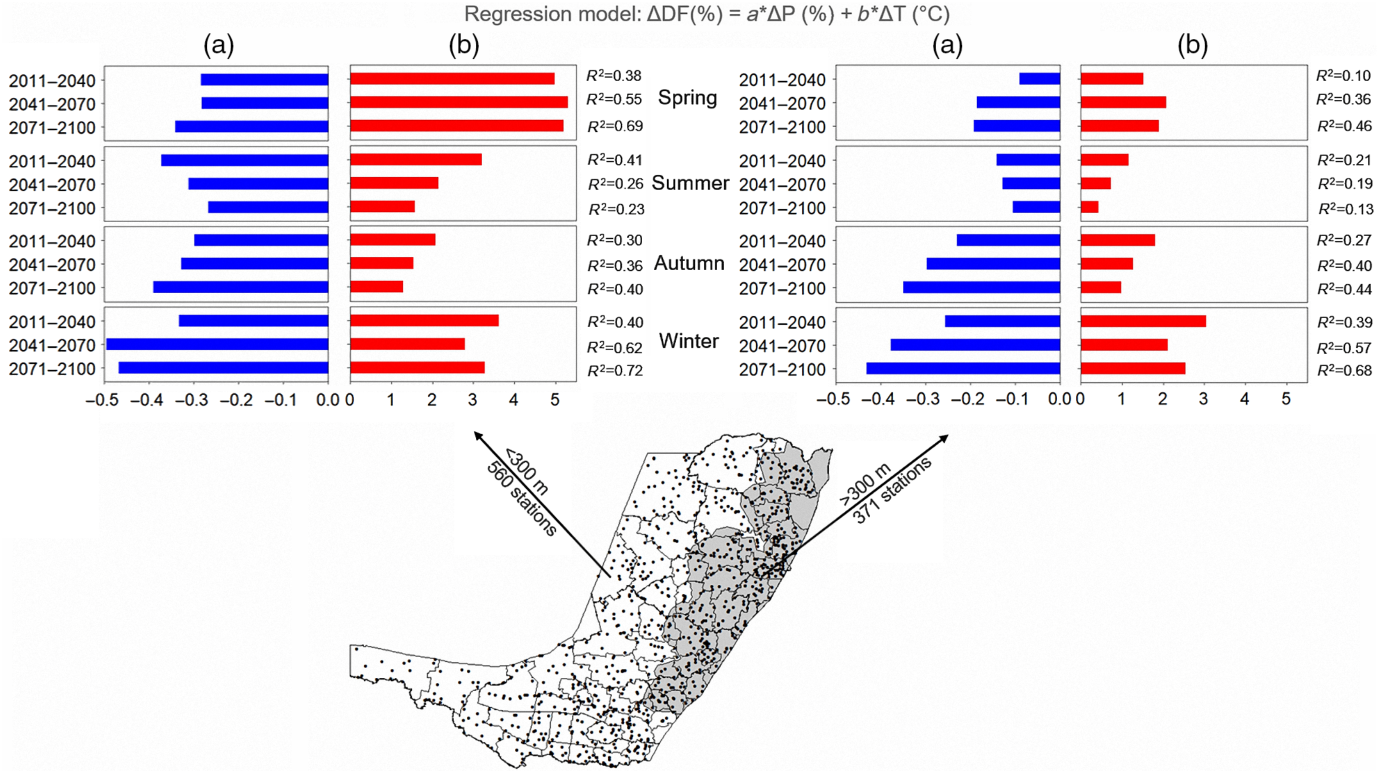

FIGURE 8 Regression analysis of the impacts of temperature (a) and precipitation (b) on drought frequency (DF, %) in the western (left) and the eastern (right) zones of the New South Wales wheat belt of southeastern Australia. Changes of DF, averaged annual total precipitation (*P*) and annual mean temperature (*T*) were first calculated for three, 30-year periods (2011–2040, 2041–2070, and 2071–2100) relative to 1961–1990 for each weather station within the western (n = 560) and eastern (n = 371) zones for all the GCMs. Least-squares multiple regression model ($\Delta DF = a^*\Delta P\ (\%) + b^*\Delta T\ (°C)$) was then built in both zones for each season and each period. All the regression coefficients (R^2) shown were significant ($p < .05$) [Colour figure can be viewed at wileyonlinelibrary.com]

emphasized that winter and spring are key growth periods for winter crops such as wheat and canola. Previous studies have shown that in dryland agriculture of southeastern Australia, precipitation declines can be amplified 1.5–1.7 times in wheat yield losses (Dijk *et al*., 2013). In our study, the projected increase of spring and winter droughts would inevitably cause decreased yields and increased risks to cropping systems in the study area. In addition, as the Australian climate is highly variable (Potgieter *et al*., 2012), the increasing trends would likely be accompanied by dramatic fluctuation as inter-annual extremely dry conditions occur more frequently (Alexander and Arblaster, 2017).

The spatial trends in drought vulnerability corresponded with temporal trends in drought. Spring and winter drought vulnerable areas were likely to expand remarkably (Figure 7). Historically, the western zone of the wheat belt was typically a drought vulnerable area due to lower precipitation and higher temperature (Figure 2). Crop yields in these areas were typically lower compared to the eastern areas (Hochman *et al*., 2016). Our results showed that drought prone areas were likely to increase, which meant that the areas of low-level crop yield would expand. By 2100, more than half of the wheat belt was expected to have low crop yields or might not be suitable for growing winter cereal crops. On the other hand, summer and autumn drought prone areas were primarily in the southwest and northwest and might only experience slight changes (Figures 6 and 7). This could be attributed to the increases of projected precipitation during summers and autumns in the late decades of the 21st century (Figure S3).

In general, spatial and temporal increases in drought events were primarily driven by decreased precipitation and also evaporation through increased temperatures (Sheffield and Wood, 2007). It is commonly recognized that climate change will cause changes in temperature and precipitation all over the world (Pachauri and Meyer, 2015). An absolute amount of change in precipitation or temperature may result in distinctly different changes in drought conditions in different climate regions. Our results demonstrated that temperature and precipitation possessed greater ability to regulate the aridity condition in traditional drought prone areas. A similar decrease in precipitation or increase in temperature would cause a greater increase in drought frequency in dry areas compared to wet areas (Figure 8). This creates a challenge for historically dry areas in face of climate change. In the future, a slight increase in temperature or decrease in precipitation will inevitably increase the risk of drought, thereby reducing the agricultural production capacity.

Our results also showed that areas of projected increased precipitation were also at risk of increased drought frequency. For example, in autumn, most of the NSW wheat belt was projected to receive more rain after 2041 (Figure S3). However, the area vulnerable to drought in autumn would still increase (Figure 7). This was mainly because the slight increase in precipitation might not fully compensate the increasing water demand caused by the increasing temperature (Liu *et al*., 2017). In addition to this, climate projections have shown that future precipitation is likely to be characterized by low frequency, high intensity, and uneven intra-annual precipitation distribution (Bao *et al*., 2017). More intense precipitation events may result in increased runoff (Trenberth *et al*., 2014) without replenishment of soil moisture. In this case, while summer precipitation amount might increase significantly (Figure S3), aridity was projected to remain relatively high. Therefore, areas with projected increased precipitation might also experience drought conditions. In addition, current drought indices which only consider the amount of precipitation are of limited utility when evaluating actual drought conditions. A more comprehensive drought index that not only considers precipitation amount but also takes into account of precipitation frequency and intensity is urgently needed for the evaluation of future drought.

The rSPEI used in our study, nevertheless, had proved to be a useful index in assessing regional drought conditions. Generally, studying drought at regional scales can better discern local characteristics of drought, resulting in a more accurate projection of drought conditions (Sheffield *et al*., 2009). The rSPEI can help achieve this goal by detecting relative drought prone areas within a particular region. The values of the rSPEI are uniquely associated with the set of weather series at all stations rather than at a single station. In this way, the rSPEI provides an objective and effective quantification of the relative intensity of drought events and their frequency with regard to the whole region (Trnka *et al*., 2009; Marcos-Garcia *et al*., 2017). Thus, the results can assist stakeholders to develop regionally specific adaptation strategies and disaster response measures. It would be worthwhile to employ the rSPEI presented here to access other drought prone areas to extract more generalized conclusions.

In addition, even though uncertainties exist in GCMs and multi-model ensemble method, results from our work could be regarded as an indication of the very likely future. Mitigation and adaptation strategies should be prepared in advance in order to minimize the adverse effects of future severe droughts on crop production. Our results showed that the NSW wheat belt was really a climatologically diverse region, so coping strategies should be specific in different zones. For example, cropping in the western zones of the southeastern Australian wheat belt would be an increasingly risky enterprise. Therefore, changing enterprise type, for example, incorporating a livestock component, purchasing additional cropping land or moving the cropping enterprise to areas with more reliable precipitation or access to irrigation might prove alternative adaptive responses for the near future. While in the eastern zones, changing sowing dates or crop rotations, stubble management, incorporating shorter growing season varieties and even fallow, might represent adaptive responses to cope with future drought. We hope that drought projections from this work are able to provide useful information for long-term planning for stakeholders.

5 | CONCLUSIONS

Temporal and spatial characteristics of future seasonal droughts in the New South Wales wheat belt of southeastern Australia until the end of 21st century were analysed in this study based on 28 statistical downscaled GCMs. The relationship between drought frequency and temperature as well as precipitation was also examined. The major conclusions are as follows:

1. Spring and winter droughts were expected to be more severe over the wheat belt of southeastern Australia, while summer and autumn drought intensities might change little.
2. The winter and spring drought prone areas were likely to spread from west to east significantly and more than half of the wheat belt would be vulnerable to winter and spring droughts by 2100. In contrast, the summer and autumn drought prone areas were primarily in the southwest and northwest, respectively, with only slight changes and sometimes even a decrease in the future.
3. Traditionally dry areas would likely suffer a greater increase in drought frequency compared to wet areas when subjected to a same increase in temperature or decrease in precipitation.

We believe this study provides useful information for local farmers and policy makers with respect to evaluating the impacts of drought change on cropping systems in southeastern Australia. However, additional studies which for example, examining the effect of rainfall intensity in a drought index, may help to increase our confidence in accurately projecting future drought change.

ACKNOWLEDGEMENTS

The first author acknowledges the China Scholarship Council (CSC) for the financial support for his Ph.D. study. Facilities for conducting this study were provided by the New South Wales Department of Primary Industries, University of Technology Sydney, and the National Basic Research Program of China (2012CB955304). We acknowledge the World Climate Research Programme's Working Group on Coupled Modelling for producing and providing model outputs. Thanks to Dr. Ian Macadam of Climate Research

Centre and ARC Centre of Excellence for Climate Extremes, University of New South Wales, Sydney for downloading GCM data.

ORCID

Puyu Feng https://orcid.org/0000-0003-4845-9876
De Li Liu https://orcid.org/0000-0003-2574-1908
Bin Wang https://orcid.org/0000-0002-6422-5802

REFERENCES

Ahmadalipour, A., Moradkhani, H. and Svoboda, M. (2016) Centennial drought outlook over the CONUS using NASA-NEX downscaled climate ensemble. *International Journal of Climatology*, 37(5), 2477–2491. https://doi.org/10.1002/joc.4859.

Alexander, L. and Arblaster, J. (2017) Historical and projected trends in temperature and precipitation extremes in Australia in observations and CMIP5. *Weather and Climate Extremes*, 15, 34–56. https://doi.org/10.1016/j.wace.2017.02.001.

Anwar, M., Liu, D., Farquharson, R., Macadam, I., Abadi, A., Finlayson, J., Wang, B. and Ramilan, T. (2015) Climate change impacts on phenology and yields of five broadacre crops at four climatologically distinct locations in Australia. *Agricultural Systems*, 132, 133–144. https://doi.org/10.1016/j.agsy.2014.09.010.

Bao, J., Sherwood, S., Alexander, L. and Evans, J. (2017) Future increases in extreme precipitation exceed observed scaling rates. *Nature Climate Change*, 7(2), 128–132. https://doi.org/10.1038/nclimate3201.

Bartier, P. and Keller, C. (1996) Multivariate interpolation to incorporate thematic surface data using inverse distance weighting (IDW). *Computers & Geosciences*, 22(7), 795–799. https://doi.org/10.1016/0098-3004(96)00021-0.

BOM and CSIRO. (2016) State of the climate. Available at: http://www.bom.gov.au/state-of-the-climate/ [accessed 23th January 2018].

CCIA. (2015) Climate change in Australia: projections for Australia's NRM regions. Available at: https://www.climatechangeinaustralia.gov.au/en/publications-library/technical-report/ [accessed 23th January 2018].

Dai, A. (2012) Increasing drought under global warming in observations and models. *Nature Climate Change*, 3(1), 52–58. https://doi.org/10.1038/nclimate1633.

Diffenbaugh, N. and Field, C. (2013) Changes in ecologically critical terrestrial climate conditions. *Science*, 341(6145), 486–492. https://doi.org/10.1126/science.1237123.

Dijk, A., Beck, H., Crosbie, R., de Jeu, R., Liu, Y., Podger, G., Timbal, B. and Viney, N. (2013) The millennium drought in southeast Australia (2001–2009): natural and human causes and implications for water resources, ecosystems, economy, and society. *Water Resources Research*, 49(2), 1040–1057. https://doi.org/10.1002/wrcr.20123.

Dubrovsky, M., Svoboda, M., Trnka, M., Hayes, M., Wilhite, D., Zalud, Z. and Hlavinka, P. (2008) Application of relative drought indices in assessing climate-change impacts on drought conditions in Czechia. *Theoretical and Applied Climatology*, 96(1–2), 155–171. https://doi.org/10.1007/s00704-008-0020-x.

Field, C. (2012) *Managing the Risks of Extreme Events and Disasters to Advance Climate Change Adaptation*. Cambridge: Cambridge University Press.

Gao, X., Zhao, Q., Zhao, X., Wu, P., Pan, W., Gao, X. and Sun, M. (2017) Temporal and spatial evolution of the standardized precipitation evapotranspiration index (SPEI) in the Loess Plateau under climate change from 2001 to 2050. *Science of the Total Environment*, 595, 191–200. https://doi.org/10.1016/j.scitotenv.2017.03.226.

Guttman, N. (1998) Comparing the Palmer drought index and the standardized precipitation index. *Journal of the American Water Resources Association*, 34(1), 113–121. https://doi.org/10.1111/j.1752-1688.1998.tb05964.x.

Hamed, K. and Ramachandra Rao, A. (1998) A modified Mann–Kendall trend test for autocorrelated data. *Journal of Hydrology*, 204(1–4), 182–196. https://doi.org/10.1016/s0022-1694(97)00125-x.

He, L., Cleverly, J., Wang, B., Jin, N., Mi, C., Liu, D. and Yu, Q. (2017) Multi-model ensemble projections of future extreme heat stress on rice across southern China. *Theoretical and Applied Climatology*, 133(3–4), 1107–1118. https://doi.org/10.1007/s00704-017-2240-4.

Heim, R. (2002) A review of twentieth-century drought indices used in the United States. *Bulletin of the American Meteorological Society*, 83(8), 1149–1166. https://doi.org/10.1175/1520-0477-83.8.1149.

Hochman, Z., Gobbett, D., Horan, H. and Navarro, G.J. (2016) Data rich yield gap analysis of wheat in Australia. *Field Crops Research*, 197, 97–106. https://doi.org/10.1016/j.fcr.2016.08.017.

Kirono, D., Kent, D., Hennessy, K. and Mpelasoka, F. (2011) Characteristics of Australian droughts under enhanced greenhouse conditions: results from 14 global climate models. *Journal of Arid Environments*, 75(6), 566–575. https://doi.org/10.1016/j.jaridenv.2010.12.012.

Liu, D. and Zuo, H. (2012) Statistical downscaling of daily climate variables for climate change impact assessment over New South Wales, Australia. *Climatic Change*, 115(3–4), 629–666. https://doi.org/10.1007/s10584-012-0464-y.

Liu, D., Anwar, M., O'Leary, G. and Conyers, M. (2014) Managing wheat stubble as an effective approach to sequester soil carbon in a semi-arid environment: spatial modelling. *Geoderma*, 214–215, 50–61. https://doi.org/10.1016/j.geoderma.2013.10.003.

Liu, M., Xu, X., Sun, A. and Wang, K. (2017) Decreasing spatial variability of drought in southwest China during 1959–2013. *International Journal of Climatology*, 37(13), 4610–4619. https://doi.org/10.1002/joc.5109.

Lloyd-Hughes, B. and Saunders, M. (2002) A drought climatology for Europe. *International Journal of Climatology*, 22(13), 1571–1592. https://doi.org/10.1002/joc.846.

Lutz, S., Mallucci, S., Diamantini, E., Majone, B., Bellin, A. and Merz, R. (2016) Hydroclimatic and water quality trends across three Mediterranean river basins. *Science of the Total Environment*, 571, 1392–1406. https://doi.org/10.1016/j.scitotenv.2016.07.102.

Marcos-Garcia, P., Lopez-Nicolas, A. and Pulido-Velazquez, M. (2017) Combined use of relative drought indices to analyze climate change impact on meteorological and hydrological droughts in a Mediterranean basin. *Journal of Hydrology*, 554, 292–305. https://doi.org/10.1016/j.jhydrol.2017.09.028.

Mishra, A. and Singh, V. (2010) A review of drought concepts. *Journal of Hydrology*, 391(1–2), 202–216. https://doi.org/10.1016/j.jhydrol.2010.07.012.

Morid, S., Smakhtin, V. and Bagherzadeh, K. (2007) Drought forecasting using artificial neural networks and time series of drought indices. *International Journal of Climatology*, 27(15), 2103–2111. https://doi.org/10.1002/joc.1498.

Mpelasoka, F., Awange, J. and Goncalves, R. (2018) Accounting for dynamics of mean precipitation in drought projections: a case study of Brazil for the 2050 and 2070 periods. *Science of the Total Environment*, 622–623, 1519–1531. https://doi.org/10.1016/j.scitotenv.2017.10.032.

Nicholls, N. (2004) The changing nature of Australian droughts. *Climatic Change*, 63(3), 323–336. https://doi.org/10.1023/b:clim.0000018515.46344.6d.

Pachauri, R. and Meyer, L. (2015) *Climate Change 2014*. IPCC: Geneva.

Palmer, W. (1965) *Meteorological drought*, weather bureau research paper no. 45. Washington, D.C.: U.S. Department of Commerce.

Patel, N., Chopra, P. and Dadhwal, V. (2007) Analyzing spatial patterns of meteorological drought using standardized precipitation index. *Meteorological Applications*, 14(4), 329–336. https://doi.org/10.1002/met.33.

Peters, G., Marland, G., Le Quéré, C., Boden, T., Canadell, J. and Raupach, M. (2011) Rapid growth in CO_2 emissions after the 2008–2009 global financial crisis. *Nature Climate Change*, 2(1), 2–4. https://doi.org/10.1038/nclimate1332.

Pohlert, T. (2018) Trend: non-parametric trend tests and change-point detection. R package version 1.1.0. Available at: https://CRAN.R-project.org/package=trend. [accessed 23th January 2018].

Potgieter, A., Meinke, H., Doherty, A., Sadras, V., Hammer, G., Crimp, S. and Rodriguez, D. (2012) Spatial impact of projected changes in rainfall and temperature on wheat yields in Australia. *Climatic Change*, 117(1–2), 163–179. https://doi.org/10.1007/s10584-012-0543-0.

Ribeiro, B., Sales, L., De Marco, P., Jr. and Loyola, R. (2016) Assessing mammal exposure to climate change in the Brazilian Amazon. *PLOS One*, 11(11), e0165073. https://doi.org/10.1371/journal.pone.0165073.

Richardson, C. and Wright, D. (1984) *WGEN: a model for generating daily weather variables*. Washington, D.C.: U.S. Department of Agriculture, Agriculture Research Service.

Sen, P. (1968) Estimates of the regression coefficient based on Kendall's tau. *Journal of the American Statistical Association*, 63(324), 1379–1389. https://doi.org/10.2307/2285891.

Serrano-Notivoli, R., Beguería, S., Saz, M. and de Luis, M. (2018) Recent trends reveal decreasing intensity of daily precipitation in Spain. *International Journal of Climatology.*, 38, 4211–4224. https://doi.org/10.1002/joc.5562.

Shahid, S. (2010) Trends in extreme rainfall events of Bangladesh. *Theoretical and Applied Climatology*, 104(3–4), 489–499. https://doi.org/10.1007/s00704-010-0363-y.

Sheffield, J. and Wood, E. (2007) Projected changes in drought occurrence under future global warming from multi-model, multi-scenario, IPCC AR4 simulations. *Climate Dynamics*, 31(1), 79–105. https://doi.org/10.1007/s00382-007-0340-z.

Sheffield, J., Andreadis, K., Wood, E. and Lettenmaier, D. (2009) Global and continental drought in the second half of the twentieth century: severity–area–duration analysis and temporal variability of large-scale events. *Journal of Climate*, 22(8), 1962–1981. https://doi.org/10.1175/2008jcli2722.1.

Sheikhy, N.T., Aris, A., Sefie, A. and Keesstra, S. (2017) Detecting and predicting the impact of land use changes on groundwater quality, a case study in northern Kelantan, Malaysia. *Science of the Total Environment*, 599–600, 844–853. https://doi.org/10.1016/j.scitotenv.2017.04.171.

Sonmez, F., Komuscu, A., Erkan, A. and Turgu, E. (2005) An analysis of spatial and temporal dimension of drought vulnerability in Turkey using the standardized precipitation index. *Natural Hazards*, 35(2), 243–264. https://doi.org/10.1007/s11069-004-5704-7.

Spinoni, J., Naumann, G., Carrao, H., Barbosa, P. and Vogt, J. (2013) World drought frequency, duration, and severity for 1951–2010. *International Journal of Climatology*, 34(8), 2792–2804. https://doi.org/10.1002/joc.3875.

Spinoni, J., Vogt, J., Naumann, G., Barbosa, P. and Dosio, A. (2017) Will drought events become more frequent and severe in Europe? *International Journal of Climatology*, 38(4), 1718–1736. https://doi.org/10.1002/joc.5291.

Tebaldi, C. and Knutti, R. (2007, 1857) The use of the multi-model ensemble in probabilistic climate projections. *Philosophical Transactions of the Royal Society A: Mathematical, Physical and Engineering Sciences*, 365, 2053–2075. https://doi.org/10.1098/rsta.2007.2076.

Thomas, M., Nolan, D. and John, K. (1993) The relationship of drought frequency and duration to time scales. In: *Proceedings of the 8th Conference on Applied Climatology*, 17(22), 179–183. Boston, MA: American Meteorological Society.

Trenberth, K., Dai, A., Schrier, G., Jones, P., Barichivich, J., Briffa, K. and Sheffield, J. (2014) Global warming and changes in drought. *Nature Climate Change*, 4(1), 17–22. https://doi.org/10.1038/nclimate2067.

Trinh, T., Ishida, K., Kavvas, M., Ercan, A. and Carr, K. (2017) Assessment of 21st century drought conditions at Shasta Dam based on dynamically projected water supply conditions by a regional climate model coupled with a physically-based hydrology model. *Science of the Total Environment*, 586, 197–205. https://doi.org/10.1016/j.scitotenv.2017.01.202.

Trnka, M., Dubrovský, M., Svoboda, M., Semerádová, D., Hayes, M., Žalud, Z. and Wilhite, D. (2009) Developing a regional drought climatology for the Czech Republic. *International Journal of Climatology*, 29(6), 863–883. https://doi.org/10.1002/joc.1745.

Ummenhofer, C., England, M., McIntosh, P., Meyers, G., Pook, M., Risbey, J., Gupta, A. and Taschetto, A. (2009) What causes southeast Australia's worst droughts? *Geophysical Research Letters*, 36(4), L04706. https://doi.org/10.1029/2008gl036801.

Vicente-Serrano, S., Beguería, S. and López-Moreno, J. (2010) A multiscalar drought index sensitive to global warming: the standardized precipitation evapotranspiration index. *Journal of Climate*, 23(7), 1696–1718. https://doi.org/10.1175/2009jcli2909.1.

Wang, Q., Shi, P., Lei, T., Geng, G., Liu, J., Mo, X., Li, X., Zhou, H. and Wu, J. (2015) The alleviating trend of drought in the Huang–Huai–Hai Plain of China based on the daily SPEI. *International Journal of Climatology*, 35(13), 3760–3769. https://doi.org/10.1002/joc.4244.

Wang, B., Liu, D., Macadam, I., Alexander, L., Abramowitz, G. and Yu, Q. (2016) Multi-model ensemble projections of future extreme temperature change using a statistical downscaling method in southeastern Australia. *Climatic Change*, 138(1–2), 85–98. https://doi.org/10.1007/s10584-016-1726-x.

Wells, N., Goddard, S. and Hayes, M. (2004) A self-calibrating Palmer drought severity index. *Journal of Climate*, 17(12), 2335–2351. https://doi.org/10.1175/1520-0442(2004)017<2335:aspdsi>2.0.co;2.

Wilhelmi, O. and Wilhite, D. (2002) Assessing vulnerability to agricultural drought: a Nebraska case study. *Natural Hazards*, 25(1), 37–58. https://doi.org/10.1023/A:1013388814894.

Wilhite, D. (1993) *Drought Assessment, Management, and Planning*. Boston, MA: Kluwer Academic.

Zhang, X. (2005) Spatial downscaling of global climate model output for site-specific assessment of crop production and soil erosion. *Agricultural and Forest Meteorology*, 135(1–4), 215–229. https://doi.org/10.1016/j.agrformet.2005.11.016.

Zhang, X. (2007) A comparison of explicit and implicit spatial downscaling of GCM output for soil erosion and crop production assessments. *Climatic Change*, 84(3–4), 337–363. https://doi.org/10.1007/s10584-007-9256-1.

SUPPORTING INFORMATION

Additional supporting information may be found online in the Supporting Information section at the end of the article.

How to cite this article: Feng P, Liu DL, Wang B, Waters C, Zhang M, Yu Q. Projected changes in drought across the wheat belt of southeastern Australia using a downscaled climate ensemble. *Int J Climatol*. 2019;39:1041–1053. https://doi.org/10.1002/joc.5861